

CONSTRAINING THE R-MODE SATURATION AMPLITUDE FROM A HYPOTHETICAL DETECTION OF R-MODE GRAVITATIONAL WAVES FROM A NEWBORN NEUTRON STAR - SENSITIVITY STUDY

ANTONIS MYTIDIS¹ MICHAEL COUGHLIN² AND BERNARD WHITING³

Submitted for publication in The Astrophysical Journal

ABSTRACT

This paper consists of two related parts: In the first part we derive an expression of the moment of inertia (MOI) of a neutron star as a function of observables from a hypothetical r-mode gravitational wave detection. For a given r-mode detection we show how the value of the MOI of a neutron star constrains the equation of state (EOS) of the matter in the core of the neutron star. Subsequently, for each candidate EOS, we derive a possible value of the saturation amplitude, α , of the r-mode oscillations on the neutron star. Additionally, we argue that a r-mode detection will provide clues about the cooling rate mechanism of the neutron star. The above physics that can be derived from a hypothetical r-mode detection constitute our motivation for the second part of the paper. In that part we present a detection strategy to efficiently search for r-modes in gravitational-wave data. R-mode signals were injected into simulated noise colored with the advanced LIGO (aLIGO) and Einstein Telescope (ET) sensitivity curves. The r-mode waveforms used are those predicted by early theories based on a polytropic equation of state (EOS) neutron star matter (Owen et al. 1998). In our best case scenario (α of order 10^{-1}), the maximum detection distance when using the aLIGO sensitivity curve is ~ 1 Mpc (supernova event rate of 3-4 per century) while the maximum detection distance when using the ET sensitivity curve is ~ 10 Mpc (supernova event rate of 1-2 per year). Our results suggest that if aLIGO takes data in 2015, it may be possible to set constraints for the EOS of the neutron star remnant of the Messier 82 supernova (SN2014J) that occurred in January 2014. Depending on the r-mode parameters and detection sensitivity we may be able to determine an upper bound (in the worst case) on the r-mode saturation amplitude or (in the best case) determine its value based on the assumed EOS.

Subject headings: aLIGO, neutron stars, equation of state, r-modes, gravitomagnetic waves, gravitational waves, supernova, CFS instability

1. INTRODUCTION

A hypothetical detection of r-mode gravitational radiation from newborn neutron stars could have at least three major implications in our understanding of neutron stars: (i) explanation of the low rotational frequencies of the observed neutron stars when compared to their possible rotational frequencies at birth, (ii) set constraints on the equation of state of the matter in the core of the neutron star and (iii) set upper bounds on α and settle the debate about the magnitude of the saturation amplitude of the r-mode mass current oscillations on neutron stars.

After some preliminaries in section 2, the paper splits into two parts: the first part consists of sections 3-7 and the second part consists of sections 8-11. In the first part we present the physics of a neutron star that can be derived from a hypothetical r-mode detection: (i) the MOI of the neutron star, (ii) the EOS of the matter in the neutron star nucleus and (iii) the saturation amplitude (α) of the r-mode mass-current oscillations. These results constitute our motivation for the second part, to perform a sensitivity study on r-modes: using

(time-shifted) eLIGO data, recolored with aLIGO and ET sensitivity curves, we examine the distances at which our decision making algorithms can be sensitive to r-mode signals from newborn neutron stars with a False Alarm Rate (FAR) of 0.1% and a False Dismissal Rate (FDR) of 50%.

The first part of the paper is organized as follows: in section 3 we discuss the power dependence on the gravitational-wave frequency and the saturation amplitude, α , of the r-mode oscillations. This result is used in section 4 to argue that among all possible r-mode sources newborn neutron stars are the most promising sources of detectable r-mode gravitational waves. In section 5, we present the time frame after a supernova explosion in which we would expect to detect r-mode gravitational waves. We end the first part of the paper with sections 6 and 7, where we present the motivation for a r-mode gravitational-wave search. In section 6 we derive a relation between r-mode gravitational waves and the MOI of the neutron star, while in section 7 we show how this relation is used to constrain the EOS of the neutron star matter and subsequently set constraints on the saturation amplitude, α , of neutron star r-mode oscillations.

The second part of the paper is organized as follows: in sections 8 and 9 we discuss the choice of parameters used to construct the waveforms needed to design the

^{1,3} Department of Physics, University of Florida, 2001 Museum Road, Gainesville, FL 32611-8440; mytidis@phys.ufl.edu, bernard@phys.ufl.edu

² Department of Physics, Harvard University ; coughlin@physics.harvard.edu

sensitivity study. In section 8 we determine the range of possible values for the initial spindown frequency, Ω_o , of the neutron star, while in section 9 we argue about the choice of the range of values for the parameter α . These 2 parameters determine the waveforms used in the sensitivity study presented in sections 10 and 11. In section 10 we present our choice of waveforms and plot several of them demonstrating the frequency spin-down dependence on α and f_o , while in section 11 we present the method of waveform injection and recovery as well as the results we obtained on the detection distances for each waveform that was used. The paper ends with a discussion on the results from our sensitivity study as well as suggestions for future work that will follow in a second paper.

2. PRELIMINARIES

In the late 1990's, the r-mode toroidal pulsations of a neutron star became very promising for generating strong gravitational-wave signals due to the Chandrasekhar-Friedman-Schutz (CFS) instability they exhibit (Friedman & Schutz 1978a,b). R-modes of any harmonic, frequency and amplitude are subject to this instability at any angular velocity of the star (Andersson 1998; Friedman & Morsink 1998). Therefore, even the smallest toroidal perturbations in the velocity of the neutron star mass currents will keep increasing in amplitude. Since the energy source of the r-mode oscillations is the rotational energy of the star, these small perturbations can eventually reach energy values of the order of the rotational energy of the neutron star. That would imply that all neutron stars are unstable and would contradict our observations. Therefore, some r-mode damping mechanism must be active resulting in the r-mode oscillation reaching a saturation amplitude, thus preserving the stability of the neutron star.

In considering the saturation amplitude, its normalization is such that values of order 1 carry energy of the same order of magnitude as the total rotational energy of the neutron star. Some authors have introduced damping mechanisms that can cause saturation at r-mode oscillation amplitudes of order $10^{-4} - 10^{-2}$ dimensionless units (Bondarescu et al. 2009), while others have introduced mechanisms that cause saturation at amplitudes equal to or larger than 10^{-1} (Alford et al. 2012). On the other hand, some studies have examined the hypothesis that, under certain conditions, r-mode oscillations may get suppressed when neutron star models with a solid crust are considered (Lindblom et al. 2000). In this case, the r-modes would be completely suppressed when the temperature of the neutron star drops below 10^8 °K. However, we are interested in the very early stages in the life of a newborn neutron star, when its core temperature is still around $10^9 - 10^{10}$ °K. Therefore, this solid-core suppression, if it exists, does not come into play until much later on in the evolution of the neutron star. The uncertainty exemplified in this situation calls for the design of a search for a r-mode gravitational radiation from newborn neutron stars to discover their saturation amplitudes.

The Bondarescu, Teukolsky and Wasserman '09 result

was the outcome of numerous earlier studies e.g. (Brink et al. 2004) that discovered a coupling between the r-mode and other inertial modes. Bondarescu et al.'s numerical study showed that for initial amplitudes of order 10^{-6} , non-linear couplings of the r-mode with other (neighboring in frequency) inertial modes can result in saturation of the r-mode amplitude at values of order up to 10^{-2} (in their most optimistic case scenario).

If the assumptions in the Bondarescu et al. model do not hold and the r-mode does not saturate at their suggested amplitudes, a different mechanism may saturate the r-mode oscillations at higher amplitudes. Such possibilities were considered by Mark Alford et al., who worked on models where the r-mode oscillations can reach saturation amplitudes 2 to 3 orders of magnitude larger than those predicted by Bondarescu et al. They explored mechanisms that can saturate the r-mode oscillations at amplitudes of order $10^{-1} - 1$ (Alford et al. 2012). They discovered that non-linear bulk viscosity will cause r-modes to saturate at large amplitudes and spin down the neutron star in much shorter time scales than Bondarescu et al. had suggested.

3. ENERGETICS

In this section we present the expression for the r-mode waveforms that was derived in (Owen et al. 1998) specifically for neutron star matter obeying a polytropic EOS. We then derive the power dependence on the r-mode gravitational wave frequency, and the saturation amplitude α . This is used in section 4 where we argue that newborn neutron stars are the most promising sources for r-mode gravitational waves.

3.1. Frequency evolution and energy of the r-mode oscillation

Though very simplistic, the Owen et al. '98 model is still a very good approximation for the early stages of the neutron star spin-down (Owen et al. 1998). More complicated numerical methods have shown that a r-mode saturation amplitude $\alpha = 10^{-2}$ can result in a spin-down whose energy loss can be detected as gravitational radiation by aLIGO (Bondarescu et al. 2009). When this saturation amplitude is used in the '98 model, we see that there is a good agreement in the angular velocity evolution of the neutron star up to several months after the start of the neutron star spin-down. The evolution of the angular velocity Ω of the neutron star in the Owen et al. '98 model is described by

$$\frac{d\Omega}{dt} = \frac{2\Omega}{\tau_{GR}} \frac{\sigma Q}{1 - \sigma Q} \quad (1)$$

with $\sigma = \alpha^2$, where α is the amplitude at which the r-mode oscillation saturates, Q is a dimensionless equation of state dependent parameter that takes the value $Q = 9.4 \times 10^{-2}$ for the polytropic neutron star model and τ_{GR} is the gravitational radiation (e-folding) time scale and is given by

$$\frac{1}{\tau_{GR}} = \frac{1}{\tilde{\tau}_{GR}} \left(\frac{\Omega^2}{\pi G \tilde{\rho}} \right)^{l+1} \quad (2)$$

where G is the gravitational constant and $\bar{\rho}$ is the average density of the neutron star (Owen et al. 1998). Combining (1) and (2) for $l = 2$, $\tilde{\tau}_{GR} = -3.3$ s and neglecting terms with powers of σQ higher than 1 we get

$$\frac{d\Omega}{dt} = -\frac{2\lambda Q}{3.3} \frac{\Omega^7}{(\pi G \bar{\rho})^3} \quad (3)$$

where $\lambda = \sigma s^{-1}$. Integrating (3) we get the angular velocity evolution of the neutron star to be

$$\Omega(t) = \frac{\Omega_o}{\left(1 + \frac{12\lambda Q}{3.3} \left(\frac{\Omega_o^2}{\pi G \bar{\rho}}\right)^3 t\right)^{\frac{1}{6}}} \quad (4)$$

where Ω_o is the angular velocity at birth. An extension of this model that includes magnetic braking effects, is described in (Ho & Lai 2000) and (Staff et al. 2012). From (4), we can derive the time evolution of the neutron star rotational frequency (with f_o being the initial frequency) to be

$$f(t) = \frac{f_o}{\left(1 + \frac{12(2\pi)^6 \lambda Q}{3.3} \left(\frac{f_o^2}{\pi G \bar{\rho}}\right)^3 t\right)^{\frac{1}{6}}} \quad (5)$$

Dividing numerator and denominator of the right hand side by f_o we get

$$f(t) = \frac{1}{\left(\frac{1}{f_o^6} + \frac{7.3 \times 10^3 \lambda Q}{(G \bar{\rho})^3} t\right)^{\frac{1}{6}}} \quad (6)$$

which results in

$$f(t) = \frac{1}{(f_o^{-6} + \mu t)^{\frac{1}{6}}} \quad (7)$$

$$\mu = 1.1 \times 10^{-20} |\alpha|^2 \frac{\text{s}^{-1}}{\text{Hz}^6} \quad (8)$$

and the time needed for the neutron star rotational frequency to evolve from some initial frequency f_o to a frequency value $f < f_o$ (using $f_o^6 \gg f^6$) is given by

$$t \simeq \frac{93}{|\alpha|^2} \left(\frac{1 \text{kHz}}{f}\right)^6 \text{ s} \quad (9)$$

The Owen et al '98 model depends on two parameters: the initial angular velocity $\Omega_o = 2\pi f_o$ discussed in section 2 and the r-mode oscillation saturation amplitude α . Using the upper bound of the angular velocity $\Omega_{ns} \simeq 7.2 \times 10^3 \text{ rad s}^{-1}$ (discussed in section 8.1) we conclude that we can take $f_o \simeq 1.1 \times 10^3 \text{ Hz}$. Since the r-mode gravitational wave frequency, f_{gw} , is related to the neutron star rotational frequency, f_{ns} , by $f_{gw} = 4/3 f_{ns}$ we conclude that r-mode gravitational waves from newborn neutron stars would have initial frequencies bounded above by $f_{gw} \simeq 1.5 \times 10^3 \text{ Hz}$.

Estimating the value of the parameter α is not as easy as estimating f_o . During the decade following the '98 paper there was no known mechanism that could stop the r-mode amplitude from growing

Teukolsky (red) vs Owen (blue) model with alpha=0.01 for a spinning down ns

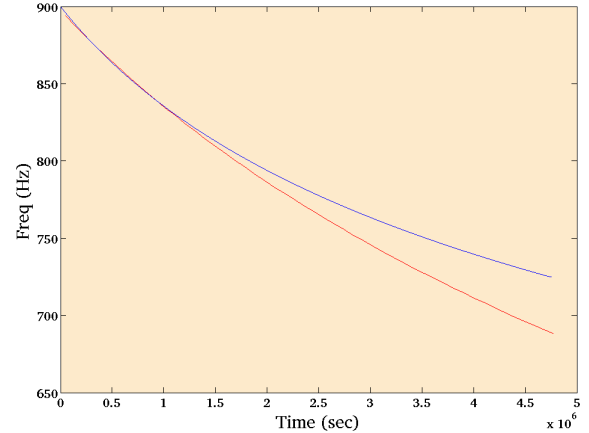


FIG. 1.— R-mode waveform (red) predicted by the best case scenario of Bondarescu et al. numerical simulations where the r-mode oscillations saturate at an amplitude α of order 10^{-2} . For comparison this is plotted on the same axes with the waveform described by the Owen et al. model with $\alpha = 10^{-2}$. The two waveforms are in a very close agreement during the early stages (up until $\sim 10^6$ s) of the frequency evolution. This is a good indication that even though the Owen et al. model is very simplistic and deviates from complicated numerical simulations for the total duration of the spin-down, it may be very accurate for the early stages of the frequency spin-down. In our sensitivity study we used 2.5×10^3 s waveforms from the Owen et al model.

due to the CFS instability. Therefore, the r-mode saturation amplitude was assumed to take values of order 1.

This is not the case in later simulations (Bondarescu, Teukolsky, Wasserman, 2009) where the r-mode oscillations exhibit non-linear couplings with daughter modes and the saturation amplitude (α) reaches maximum values of order $10^{-3} - 10^{-2}$. The models that predict these saturation amplitudes are discussed in section 9.1. Data from the Bondarescu et al. model have been obtained and a comparison of the two evolutions (both cases with $\alpha = 10^{-2}$) is given in Fig.1.

To estimate the energy stored in a neutron star r-mode and the power radiated as r-mode gravitational waves we need to know the values of f_{gw} and α . From Owen et al. '98 (Owen et al. 1998) the energy of the $l = 2$ r-mode (with $M = 1.4$ solar masses, $R = 12$ km) is given by

$$E_r = 0.82 \times 10^{-2} |\alpha|^2 M R^2 \Omega^2 = 1.3 \times 10^{38} f_{ns}^2 |\alpha|^2 \quad (10)$$

and using $f_{gw} = 4/3 f_{ns}$ we find

$$E_r = 0.73 \times 10^{38} f_{gw}^2 |\alpha|^2 \quad (11)$$

For $f_{ns} = 1.5 \times 10^3 \text{ Hz}$ and $\alpha = 1$ we find that the energy of the r-mode of a newborn neutron star is of order 10^{51} ergs.

3.2. Power dependence on the r-mode radiation frequency and saturation amplitude α

The gravitational-wave amplitude h_o of a signal with frequency $f_{gw} = f$ at a distance d and power radiated \dot{E} is given by (Bondarescu et al. 2009)

$$h_o^2 = \left(\frac{5G}{2\pi^2 c^3} \right) \left(\frac{1}{d^2} \right) \left(\frac{1}{f^2} \right) \dot{E} \quad (12)$$

(in mks units) or

$$h_o^2 \sim 6.3 \times 10^{-37} \left(\frac{1}{d^2} \right) \left(\frac{1}{f^2} \right) \dot{E} \quad (13)$$

The gravitational-wave amplitude at a distance d , the gravitational-wave frequency and the r-mode oscillation amplitude α are related by (Ho & Lai 2000)

$$h_o \approx 1.5 \times 10^{-23} \left(\frac{1\text{Mpc}}{d} \right) \left(\frac{f}{1\text{kHz}} \right)^3 |\alpha| \quad (14)$$

Substituting (14) in (13), we get a relation between the r-mode amplitude, the frequency of gravitational radiation and the power radiated in r-mode gravitational waves

$$\dot{E} \approx 3.5 \times 10^{19} f^8 |\alpha|^2 \quad (15)$$

Since the gravitational radiation power is proportional to the 8th power of frequency we expect a very rapid decrease of the signal power. From (15), we see that by the time the frequency drops to 80% of the initial frequency, the power will drop to 2.8% of the initial power. Therefore, a 0.8×10^3 Hz signal, will have radiation power ~ 36 times less than the power of a 1.0×10^3 Hz signal and therefore, a signal to noise ratio (SNR) 36 times smaller than the SNR of a signal at 1.0×10^3 Hz. This means that we are more interested in the initial stages of the spin-down.

The duration of the signal when frequency drops from 1.0×10^3 Hz to 0.8×10^3 Hz ranges from about 3.5×10^2 s for $\alpha = 1$ to about 3.5×10^6 for $\alpha = 10^{-2}$ (derived using (9)). Because of its duration, such a signal is classified as a long-transient gravitational-wave signal. For this reason gravitational-wave searches for the r-mode signals are suitable for cross-correlation type analyses (Thrane et al. 2011).

From (15), we see that for an initial frequency of 1.0×10^3 Hz the r-mode gravitational-wave power ranges from order $\sim 10^{46}$ ergs s⁻¹ for $\alpha = 10^{-2}$, to order $\sim 10^{50}$ ergs s⁻¹ for $\alpha = 1$. These values are comparable to the power of the f-mode gravitational radiation, which is the most energetic of all neutron star oscillation modes. Using the energy stored in the neutron star f-mode as given in (de Araujo et al. 2005), with order ranging from 10^{48} ergs to 10^{50} ergs and also using the damping times of order 1.0×10^2 s, (Ferrari et al. 2003) the gravitational-wave power of these modes is of order 10^{46} ergs s⁻¹ to 10^{48} ergs s⁻¹, thus concluding that r-mode gravitational radiation may be (or better, it used to be thought of) as powerful as the neutron star's most powerful gravitational radiation.

Note that (15) cannot be taken simply by taking the time derivative of (11). This is because expression (11) is just the energy of the r-mode, and does not include the rotational energy of the neutron star itself. In the saturated phase of the r-mode evolution described

by (1), it is assumed that non-linear fluid forces are coupling the r-mode to other modes of the star in such a way that gravitational radiation is able to extract energy from the overall rotational energy of the star, not just from the r-mode. So during this phase it would not be appropriate to use (11) as the total reservoir of energy that is being radiated into gravitational waves.

4. R-MODE SOURCES

In this section we use the power dependence on f and α as expressed in (15), to argue that the newborn neutron stars are the most promising sources of detectable r-mode gravitational waves. We also discuss the relevant types of electromagnetic triggers as well as their event rates.

4.1. Comparing newborn neutron stars to other sources

Apart from newborn neutron stars there are several other sources of r-mode gravitational radiation: starquakes on isolated neutron stars (Duncan 1998), pulsar postglitch relaxation (Rezania & Jahan-Miri 2000; Clemens & Rosen 2004), accreting low mass x-ray neutron stars (LMXB) in a binary system (Bondarescu et al. 2007; Levin 1999), and oscillations of the remnant star (delayed collapse) during the merging phase (before collapsing to a black hole) of a compact binary coalescence (CBC) (Baumgarte et al. 1996; Shibata & Uryu 2000). From (15) we see that, due to their high angular velocities newborn neutron stars will emit the most powerful r-mode gravitational radiation out of all of the above sources. Even if we consider all the CBC as r-mode radiation sources (ignoring the low likelihood of a delayed collapse) the event rate is much lower than the supernova event rate (within the detection distances). The LMXB, the starquakes on neutron stars and the pulsar glitches may be more frequent events but the gravitational radiation emitted by these sources is much weaker than that (predicted to be) emitted by newborn neutron stars.

4.2. Electromagnetic Counterparts

The r-mode search from newborn neutron stars depends on electromagnetic triggers from supernova type-I and type-II explosions. From (14) we see that a r-mode detection will give an estimate for the ratio α/d . Therefore, to extract any information about the magnitude of α it is necessary to know the distance to the source. Distances to type-I supernova can be calculated using the standard candle method with an error between 5 – 10% (Branch & Tammann 1992). Distances to type-II supernovae can be calculated using the expanding photosphere method giving an error of 10 – 15% (Kirshner & Kwan 1974; Schmidt et al. 1994). Furthermore, our sensitivity study results (table 1 in section 11.1) show that aLIGO can be sensitive to r-mode signals only from newborn neutron stars within our local group of galaxies. Since distances to galaxies in our local group are already known a supernova explosion within our local group would automatically give information about the distance to the hypothetical

r-mode gravitational radiation source.

4.3. Event rates within the detection distances

Considering both supernova types together we expect 2 – 3 galactic events per century (Dragicevich et al. 1999), 1 event every 2-3 years at a distance of 5 Mpc and 1-2 events per year at a distance of 10 Mpc (Ando et al. 2005). However, the local supernova rates seem to be higher around Milky Way: In the years from 2002-2005 4 events were detected (1-2 expected) within 4 Mpc and 9 events were detected (4-8 expected) within 10 Mpc. This information suggests that in the Milky Way's neighborhood the supernova rates are higher than the predicted ones, meaning that the supernova rates around Milky Way's local volume are higher than the rates at distant typical volumes. This is a motivation to improve our detection algorithms thus increasing the detection distances and cover as much of our local group of galaxies as possible.

The latest supernova (SN2014J) occurred in January of 2014 in the galaxy Messier 82 (M82) in the nearby group of galaxies M81 and it is a type-I supernova. This galaxy is at a distance of 3.5 Mpc from the Earth. Estimates show a supernova rate in our Local group of galaxies (up to a distance of 1.5 Mpc from Earth) of 3-6 per century (Mannucci et al. 2008; Li & White 2008).

5. TIME FRAME FOR A R-MODE GRAVITATIONAL WAVE DETECTION

In this section we discuss the physics of the neutron star matter via the use of the r-mode instability window to identify the time-frame for a hypothetical r-mode detection. An electromagnetic trigger will not necessarily coincide with the emission of r-mode gravitational waves. Depending on the physics of the r-modes (saturation amplitude and dissipation forces) and also the cooling mechanism of the neutron star (that depends on the EOS of the neutron star matter) the r-mode emission may start from several minutes to up to a year after an electromagnetic trigger.

5.1. The r-mode instability survival window (temperature versus angular velocity)

In a hot, newly born neutron star, the main dissipation mechanism is due to viscous forces (Andersson & Kokkotas 2001; Kokkotas & Andersson 2001). For the simplest neutron star models, two kinds of viscosity are normally considered: bulk viscosity and shear viscosity. At high temperatures (above 10^{10} °K), bulk viscosity is the dominant dissipation mechanism while shear viscosity dominates for temperatures below 10^6 °K. Hence, there is a window between $10^6 - 10^{10}$ °K where the r-mode instability may be active.

The instability window is defined by the temperature interval in which the dominant dissipation mechanism of the r-mode oscillation is the emission of (r-mode) gravitational radiation.

The amplitude, A , of the r-mode mass current oscillations evolves like

$$A \sim \exp \left[it \left(\Omega + \frac{i}{\tau} \right) \right] \quad (16)$$

where Ω is the angular velocity of the neutron star and τ is the (e-folding) time scale of the r-mode oscillations. The above expression can be expanded as

$$A \sim \exp(i\Omega t) \exp\left(-\frac{t}{\tau_g}\right) \exp\left(-\frac{t}{\tau_s}\right) \exp\left(-\frac{t}{\tau_b}\right) \quad (17)$$

where g stands for dissipation due to gravitational-wave emission, s stands for dissipation due to shear viscosity and b stands for dissipation due to bulk viscosity. Equations (16) and (17) imply that the imaginary part, $1/\tau$, of the frequency is given by

$$\frac{1}{\tau} = \frac{1}{\tau_g} + \frac{1}{\tau_s} + \frac{1}{\tau_b} \quad (18)$$

Assuming the r-mode mass perturbations, δv , have a time dependence that is given by (16) then the perturbation energy has a time dependence like

$$\delta v \delta v^* \sim \exp\left(-\frac{2t}{\tau}\right) \quad (19)$$

Therefore, the time derivative of the perturbation energy is given by

$$\frac{dE}{dt} = -\frac{2E}{\tau} \quad (20)$$

and the r-mode instability condition can be expressed by

$$\frac{1}{\tau} < 0 \quad \text{or} \quad \frac{1}{\tau_g} + \frac{1}{\tau_s} + \frac{1}{\tau_b} < 0 \quad (21)$$

The conditions given by (21) imply that the energy of the r-mode increases with time. Since τ_s and τ_b are always positive then τ_g has to be negative and smaller than τ_s and τ_b such that

$$\left| \frac{1}{\tau_g} \right| > \frac{1}{\tau_s} + \frac{1}{\tau_b} \quad (22)$$

for the r-mode instability to take place. In general $1/\tau$ is given in terms of the angular velocity of the neutron star Ω and its temperature T (Owen et al. 1998). Thus, the equation $1/\tau = 0$ defines a curve of $\Omega_{critical}(T)$. Above this curve, the instability condition is satisfied, therefore, this $\Omega_{critical}(T)$ curve defines the window over which r-mode instability will occur as seen in Fig.2.

Bulk viscosity arises because of the pressure and density variations due to the r-mode oscillation driving the fluid away from beta equilibrium. Neutrinos carry away the r-mode oscillation energy lost during this process. The balance between neutrino cooling and viscous heating plays an important role in the spin-down evolution of a neutron star (Bondarescu et al. 2009). Also, the bulk viscosity can be strongly affected by the presence of hyperons in the neutron star core. In the

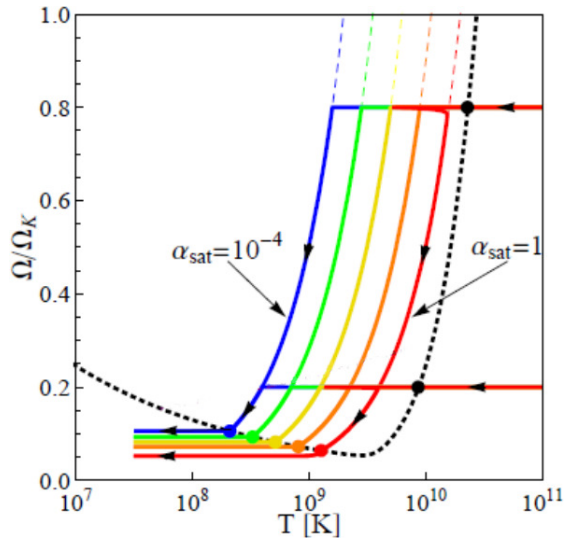


FIG. 2.— Instability window of the r-mode: The neutron stars are born with temperatures of the order $10^{11} - 10^{12}$ °K. At high temperatures (above 10^{10} °K) bulk viscosity is the dominant dissipation mechanism. Shear viscosity dominates for temperatures below 10^6 °K. Hence there is a window between $10^6 - 10^{10}$ °K where the r-mode instability is active and can have an astrophysically significant role (Kokkotas & Andersson 2001). The dotted curve defines the boundary $\Omega_{critical}(T)$ of the instability region, the dashed curves (mostly hidden underneath the solid curves) represent the steady state, heating = cooling, and the solid lines show the numerical solution of the evolution equations for two fiducial initial rotational frequencies $\Omega = 0.8\Omega_K$ and $\Omega = 0.2\Omega_K$. As shown above, the higher the α value is the sooner the initial cooling phase will merge with the corresponding steady state curve. The above image is taken from (Alford & Schwenzer 2012).

presence of hyperons the bulk viscosity coefficient is stronger and therefore, hyperon bulk viscosity becomes relevant at lower temperatures (Kokkotas & Andersson 2001).

Shear viscosity (Andersson & Kokkotas 2001; Kokkotas & Andersson 2001) is used to describe in a macroscopic manner the scattering events associated with momentum transfer. Neutron-neutron scattering provides the most important contribution in a neutron star. However, in cases the core of the neutron star becomes superfluid, electron-electron scattering is the dominant effect that contributes to the shear viscosity. Therefore, a superfluid neutron star core can affect the spin-down evolution.

5.2. Detection window after a supernova

A neutron star is born with core temperatures of $\sim 10^{12}$ °K. Right after the catastrophic collapse, the formation of a protoneutron star is defined as the collapsed star with neutrinos trapped inside its core. About 1.0×10^2 s after the collapse these neutrinos are released leading to a dramatic temperature drop to 10^{10} °K (Lattimer & Prakash 2007). The transition from a neutrino-opaque protoneutron star core to a neutrino-transparent core, resulting in the neutrino burst observed during a supernova, signals the death of the protoneutron star and the birth of a neutron star.

After the newborn neutron star enters the instability window, it undergoes an initial cooling. The spin-down

starts after the steady state (cooling=heating) curve is reached. Depending on the saturation amplitude and the EOS, this can be reached at temperatures anywhere between $10^9 - 10^{10}$ (Alford & Schwenzer 2012). That means the spin-down may start right after the neutrino burst (1.0×10^2 s after the collapse of the star) or up until the neutron star cools down to 10^9 °K. This time depends on the cooling rate of the neutron star.

The modified Urca process (MUP) can decrease the temperature of the neutron star from $T = 10^{10}$ °K to 10^9 °K in about a year and down to 10^8 °K within a million years. However, if the direct Urca process (DUP) is doing the cooling, the core temperature will drop to 10^9 °K within minutes and then drop down to 10^8 °K within days (Yakovlev & Pethick 2004). The EOS determines which cooling evolution, $T(t)$, the neutron star will follow. For a given EOS, the transition rate from slow to fast cooling occurs in a given mass range. This range is very narrow because of the sharp neutron core mass density threshold for the direct Urca process to take place (Yakovlev et al. 1999).

The growth timescale of the r-mode after it enters the instability window is of the order of ~ 40 s. Therefore, within 10 minutes the amplitude may grow up to order of 1 if not saturated before that. As saturation is reached the r-mode gravitational radiation will equilibrate at a particular heating=cooling curve (Fig.2). How long after the birth of the neutron star will this take place? From the above paragraphs we see that, depending on the equation of state and the r-mode saturation amplitude, the spin-down of a newborn neutron star may start anywhere from a few minutes up to \sim years after the neutron star is born. Therefore we conclude that if aLIGO takes data in 2015, it may be possible to set some constraints for the EOS of the neutron star remnant of the Messier 82 supernova (SN2014J) that occurred in January 2014.

6. MOTIVATION FOR THE R-MODE SENSITIVITY STUDY: MOI OF A NEUTRON STAR FROM A R-MODE GRAVITATIONAL WAVE DETECTION

In this section we derive a generalization of the r-mode waveform (6) so that the frequency evolution is expressed in terms of any EOS. We then derive an expression for the MOI of the neutron star as a function of the r-mode gravitational-wave observables, \dot{E} , \dot{f} and f . Subsequently we show how the value of the MOI sets constraints on the possible EOS of the neutron star matter. This result is used in section 7 where we derive an expression for the saturation amplitude, α , as a function of the EOS. Using this expression, a set of possible values of α can be derived, thus setting an upper bound for α .

6.1. Estimating the moment of inertia of a neutron star from a hypothetical r-mode detection

In section 2 we have assumed a polytropic EOS for the neutron star matter. The constant μ in (8) as well as the waveforms expressed in (6) are dependent on this EOS. Therefore, a hypothetical r-mode detection would

set upper bounds on the r-mode saturation amplitude α based on the assumed EOS. Using the same hypothetical detection two different EOS may result in two different upper bounds for α .

In what follows, we derive an EOS-dependent and α -independent expression (37) or (38) (which turns out to be the moment of inertia of the neutron star) that can be evaluated from a r-mode detection. Thus we conclude that a hypothetical r-mode detection can constrain the EOS of the neutron star matter and can also set upper bounds on the values of α for each permitted EOS.

In this section we seek a generalization of the spin-down formula in (Owen et al. 1998), so that no assumptions are made for the equation of state (EOS) of the neutron star matter. The gravitational radiation time scale is given by

$$\frac{1}{\tau_{gw}} = -\lambda_m MR^{2m} \Omega^{2m+2} \tilde{J}_m \quad (23)$$

where

$$\lambda_m = \frac{32\pi G}{c^{2m+3}} \left(\frac{(m-1)^m}{(2m+1)!!} \right)^2 \left(\frac{m+2}{m+1} \right)^{2m+2} \quad (24)$$

and

$$\tilde{J}_m = \frac{1}{MR^{2m}} \int_0^R \rho(r) r^{2m+2} dr \quad (25)$$

The energy E_m of the r-mode is given by

$$E_m = \frac{1}{2} \alpha^2 \Omega^2 MR^2 \tilde{J}_m \quad (26)$$

The rate of change of the energy of the r-mode oscillation is given by

$$\dot{E}_m = -\frac{2E}{\tau_{gw}} \quad (27)$$

and hence from (23), (26) and (27) we obtain

$$\dot{E}_m = \lambda_m \alpha^2 M^2 R^{2m+2} \Omega^{2m+4} \tilde{J}_m^2 \quad (28)$$

During the saturated non-linear phase of the evolution, when the r-mode oscillation has a fixed amplitude and energy, (28) gives the power of the mode being radiated as r-mode gravitational radiation. During this phase the main contribution to the r-mode is the $m = 2$ harmonic and the angular velocity of the star evolves according to (Owen et al. 1998)

$$\dot{\Omega} = \frac{2\Omega}{\tau_{gw}} \left(\frac{\alpha^2 Q}{1 - \alpha^2 Q} \right) \approx \frac{2\Omega \alpha^2 Q}{\tau_{gw}} \quad (29)$$

where the last step assumes that $\alpha^2 \ll 1$ and Q is defined by

$$Q = \frac{3\tilde{J}_2}{2\tilde{I}} \quad (30)$$

where

$$\tilde{J}_2 = \frac{1}{MR^4} \int_0^R \rho(r) r^6 dr \quad (31)$$

and

$$\tilde{I} = \frac{8\pi}{3MR^2} \int_0^R \rho(r) r^4 dr \quad (32)$$

Substituting (23), (24) and (30) in (29) (for $m = 2$) results in the EOS-dependent expression for the time evolution of the angular velocity of the neutron star

$$\dot{\Omega} = -3\lambda_2 \alpha^2 MR^4 \frac{\tilde{J}_2^2}{\tilde{I}} \Omega^7 \quad (33)$$

where $\lambda_2 = 7.7 \times 10^{-70}$. Using the result relating the angular velocity, $\omega = 2\pi f$, of the r-mode gravitational radiation to the angular velocity, Ω , of the neutron star $\omega = 4/3 \times \Omega \implies f = 2/3\pi \times \Omega$, we get the gravitational radiation frequency evolution given by

$$\dot{f} = -2.5 \times 10^{-65} MR^4 \alpha^2 \frac{(\tilde{J}_2)^2}{\tilde{I}} f^7 \text{kg}^{-1} \text{m}^{-4} \text{s}^5 \quad (34)$$

leading to the EOS-dependent r-mode radiation waveform

$$f = \left(\frac{1}{f_o^{-6} + \mu t} \right)^{\frac{1}{6}} \quad (35)$$

where

$$\mu = 1.5 \times 10^{-64} MR^4 \alpha^2 \frac{(\tilde{J}_2)^2}{\tilde{I}} \text{kg}^{-1} \text{m}^{-4} \text{s}^5 \quad (36)$$

and f_o is the initial frequency of the neutron star spin-down.

Using (28) for $m = 2$, and (33) we get the result

$$\frac{\dot{E}}{\Omega \tilde{I}} = -\frac{8\pi}{9} \int_0^R \rho(r) r^4 dr \quad (37)$$

or, in terms of the gravitational-wave frequency, f ,

$$\frac{\dot{E}}{f \dot{f}} = -2\pi^3 \int_0^R \rho(r) r^4 dr \quad (38)$$

A hypothetical r-mode detection will provide us with estimates of the model parameters f_o and μ . From these we can estimate the r-mode gravitational wave frequency, f , as well as its derivative, \dot{f} . Furthermore, from equation (12) we see that given the distance, d , to the source of the r-mode gravitational radiation, the frequency, f , of the gravitational wave and the gravitational wave strain, h , then the power, \dot{E} , of the r-mode gravitational radiation can be estimated. Therefore, we conclude that given a hypothetical r-mode gravitational wave is detected, the integral on the right hand side of (38) that gives the moment of inertia of the neutron star can be estimated.

7. CONSTRAINING THE EOS OF NEUTRON STAR MATTER AND THE R-MODE SATURATION AMPLITUDE

In this section we plot the moment of inertia versus radius and the moment of inertia versus mass representations of 17 EOS. From a hypothetical r-mode detection we can estimate the moment of inertia of the neutron star and hence estimate the possible radius and mass values for the allowed EOS. Subsequent estimates of either the radius or mass of the neutron star would further constrain the EOS. For each possible EOS we can then set upper bounds on the r-mode saturation amplitude, α . We also discuss the clues an r-mode gravitational wave detection will provide about the cooling mechanism of the neutron star.

7.1. Numerical solution to the TOV equations

Given a pair $(\rho(P), P_c)$ of an EOS and a central pressure of a neutron star we can integrate the Tolman-Oppenheimer-Volkov (TOV) equations

$$\frac{dP}{dr} = -\frac{G(\rho(P) + \frac{P}{c^2}) \left(m + \frac{4\pi r^3 P}{c^2} \right)}{r \left(r - \frac{2Gm}{c^2} \right)} \quad (39)$$

and

$$\frac{dm}{dr} = 4\pi r^2 \rho \quad (40)$$

from $r = 0..r'$ and $P = P_c..P(r')$. At every integral step we evaluate the following integrals

$$I_n(r') = \int_0^{r'} \rho(P) r^n dr \quad \text{with } n=2,4 \text{ and } 6 \quad (41)$$

which can be used to re-write (32) and (31) like

$$\tilde{I} = \frac{8\pi}{3MR^2} I_4(R) \quad \text{and} \quad \tilde{J}_2 = \frac{1}{MR^4} I_6(R) \quad (42)$$

respectively, as well as (38) like

$$\frac{\dot{E}}{ff} = -2\pi^3 I_4(R) \quad (43)$$

where R is the value of r' for which

$$P(r') = 0 \quad (44)$$

Using equation (41) with $n = 2$ and $r' = R$ we can express the total mass of a neutron star of radius R by

$$M(R) = 4\pi I_2(R) \quad (45)$$

Solving (39), (40) and (41) (for the given $\rho(P)$) while varying P_c , results in the functions $R = R(P_c)$, $I_2(R, P_c)$ and $I_4(R, P_c)$ where I_2 and I_4 are proportional to the neutron star mass and moment of inertia respectively. Using these results we can express the total mass, M , and the moment of inertia, I , of the neutron star as $M(P_c)$ and $I(P_c)$. Expressing the macroscopic observables, I , R and M in terms of the central pressure, P_c , demonstrates that the equation of state of the neutron

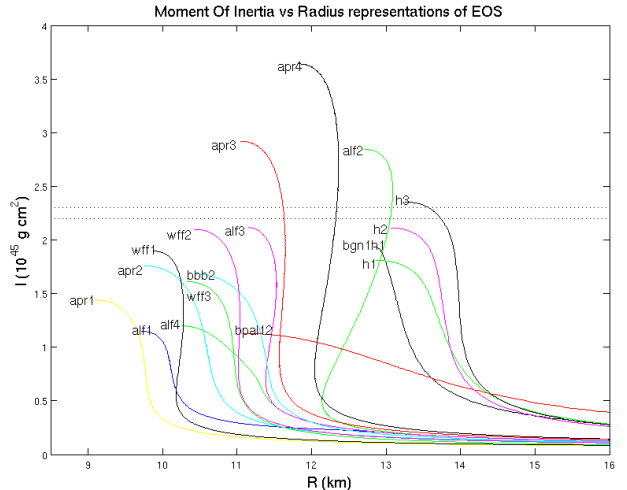


Fig. 3.— Moment of inertia versus radius representation of the EOS. The horizontal lines correspond to a range of values of the moment of inertia (estimated from a hypothetical r-mode detection), in this case $I_1 = 2.2$ and $I_2 = 2.3$. The corresponding radius range is shown in Fig.5.

star matter can be thought of as: (a) a curve in the $I - R$ plane (Fig.3), (b) a curve in the $I - M$ plane (Fig.4) and (c) a curve in the $M - R$ plane (Fig.5); all curves being parametrized by P_c , with each P_c value corresponding to a unique point on each curve. Figures 3, 4 and 5 were plotted by integrating the TOV equations using the Runge-Kutta method for a set of 17 equations of state.

A hypothetical r-mode gravitational-wave detection, with r-mode waveform parameters f_o and μ , will give an estimate of the moment of inertia, I ($\propto I_4$), of the neutron star and hence intersect the corresponding $I - R$ and $I - M$ curves. The points of intersection represent the set of all possible mass and radius values allowed by the estimated value of I . The mass and radius values are shown in (Fig.3) and (Fig.4). Using these figures we see that a subsequent measurement of either the mass or the radius of the neutron star, would pick a single $I - R$ or $I - M$ curve and hence fix a choice of the EOS. The pairs of all possible (M_i, R_i) points (i corresponding to each intersection point in (Fig.3) and (Fig.4)) are shown in (Fig.5) which is the standard $M - R$ representation of the EOS.

Upon constraining the EOS to a few options we can substitute the corresponding values of \tilde{I} , \tilde{J}_2 and R as given by (42) and (44) respectively in (36) to get

$$\mu = 3.0 \times 10^{-66} \frac{\alpha^2 (I_6(R))^2}{R^2 (I_4(R))} \quad (46)$$

Rearranging (46) we can express α as a function of the value of μ estimated from the hypothetical r-mode detection and the allowed EOS as follows

$$\alpha = 5.8 \times 10^{32} \frac{R \sqrt{\mu I_4(R)}}{I_6(R)} \quad (47)$$

Therefore, we can set constraints (for each allowed EOS) on the r-mode saturation amplitude.

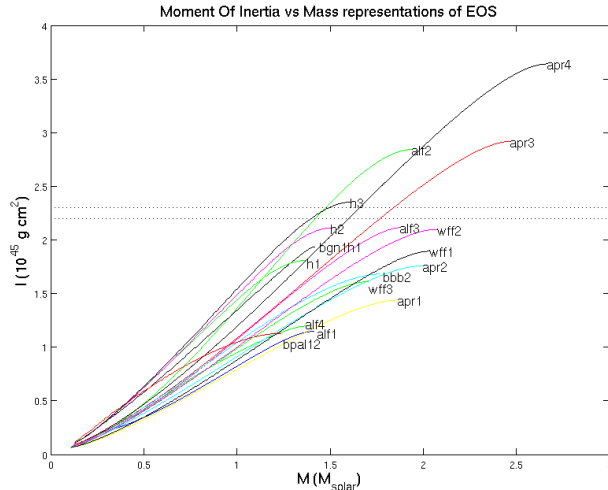


FIG. 4.— Moment of inertia versus mass representation of the EOS. The horizontal lines correspond to a range of values of the moment of inertia (estimated from a hypothetical r-mode detection), in this case $I_1 = 2.2$ and $I_2 = 2.3$. The corresponding mass range is shown in Fig.5.

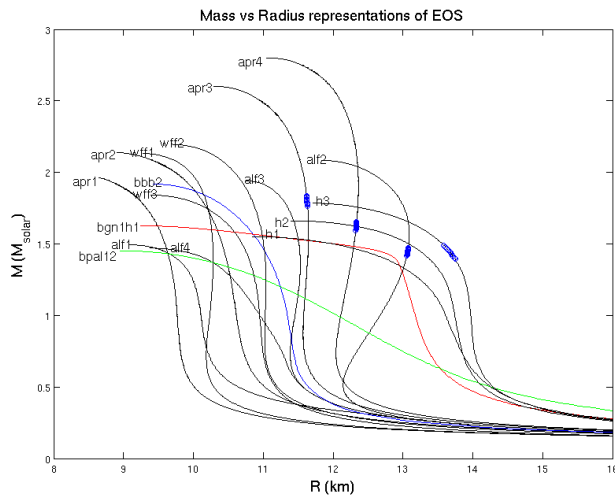


FIG. 5.— Mass versus radius representation of the EOS. Each value of the moment of inertia determined by a hypothetical r-mode detection corresponds to a point on one (or more) M - R curves. A range of moment of inertia values would correspond to a part of the M - R curves. Depending on what EOS curves are cut by the horizontal lines in Fig.3 and Fig.4 constraints may be put on what the possible EOS are for the neutron star matter.

7.2. EOS, α and the cooling rate of the neutron star

After the proton-neutron star core becomes transparent to neutrinos, the cooling mechanism (and hence the time at which the neutron star hits the heating=cooling curve) depends on the EOS of neutron star matter. For non-superfluid neutron stars there are two distinct and well known cooling mechanisms: fast neutrino cooling via the direct Urca process (DUP) and slow neutrino cooling via the modified Urca process (MUP). For a given EOS there is a density threshold, ρ_{th} , beyond which DUP can occur. For the given EOS, there is a total mass threshold, M_{th} , required for the central

density ρ_c to be equal to ρ_{th} . Neutron stars of total mass below M_{th} can only cool through MUP.

The cooling evolution splits into two universal categories: the (slow) cooling for neutron stars of mass less than the threshold mass, M_{th} , and the (fast) cooling for neutron stars of mass greater than the threshold mass, M_{th} . The cooling curves in each category are universal i.e. they are independent of the mass or EOS.

Assume the neutron star is born with an angular velocity Ω_o that stays approximately constant (ignoring magnetic braking) until the r-mode gravitational radiation starts spinning down the neutron star. A hypothetical r-mode detection will provide us with the value of Ω_o as well as with the value of μ as shown in (46). This value of μ together with the chosen EOS can be used to determine the saturation amplitude α which in turn can be used to determine the heating=cooling curve as shown in Fig.2. The horizontal line $\Omega = \Omega_o$ intersects the heating=cooling curve at $T = T_r$ and hence T_r , the temperature at which the neutron star starts spinning down due to r-mode gravitational radiation, can also be estimated.

The time, t_r , at which the neutron star temperature is equal to T_r can be estimated by the initial detection time of the r-mode gravitational radiation. Furthermore, the time, t_o , at which the neutron star is born is given by the time at which the neutrino burst occurs and may also be detected. Since the temperature of the neutron star at birth is generically approximately equal to 10^{10} °K, t_o gives the time at which the neutron star has this temperature.

The time elapsed between t_r and t_o provides the time taken for the neutron star temperature to drop from $\sim 10^{10}$ °K to T_r . Therefore, the neutron star cooling rate can be estimated. This cooling rate may be consistent either with DUP (total mass has to be above M_{th}) or MUP (total mass has to be below M_{th}). If the cooling mechanism (implied by the cooling rate) is not consistent with the mass of the neutron star (implied by the chosen EOS) that means the chosen EOS is not the correct one.

Constraining the EOS of a neutron star using cooling mechanism considerations as well as the value of the MOI of the neutron star (as predicted by a hypothetical r-mode detection) together with equations (46) and (47) are the main results of the first part of the paper. These results demonstrate the importance of a hypothetical r-mode detection as a source of information about the physics of the state of matter in the interior of the neutron star as well as the neutron star mass-current oscillations.

This information carried by r-mode gravitational waves constitutes the motivation for the second part of the paper: to perform a sensitivity study on r-mode signals from newborn neutron stars. This study starts with section 8, where we first determine the characteristics of a set of representative waveforms that were injected on background detector noise and then recovered using a

clustering algorithm.

8. WAVEFORM PARAMETERS: RANGE OF POSSIBLE VALUES OF f_o

In the sections that follow we are performing a sensitivity study to examine the distances at which the aLIGO and ET detectors (combined with the preprocessing and decision making algorithms) will be sensitive for such signals. To perform the sensitivity study we need to choose a representative set of waveforms whose choice depends on the range of values of the waveform parameters, f_o and α . To cover the whole spectrum of possibilities we need to determine the highest theoretically possible rotational velocities of neutron stars at birth and also determine the highest theoretically possible values of α . In this section we determine the possible range of values for the rotational velocity of neutron stars at birth.

8.1. Theoretical upper bound for the neutron star angular velocity at birth

The observed neutron star angular velocities are up to 25 times less than the theoretical upper bound of angular velocities that neutron stars may possess at birth. Conservation of angular momentum of the progenitor star results in much higher angular velocities at birth than those our observations reveal. Therefore, there must be a mechanism that causes the neutron star to spin down to the observed angular velocities.

A progenitor mass between 8 and 25 solar masses will result in a supernova with a neutron star as a remnant. Numerical evolutions (Heger et al. 2003) have shown that such progenitors reach angular velocities very close to the critical ones (called Kepler angular velocities) at which the stars would fall apart due to centrifugal forces. Three different approaches (general relativistic with and without differential rotation as well as numerical evolution of a pre-supernova stellar model) point towards an upper bound of $7.2 \times 10^3 \text{ rad s}^{-1}$ for the critical angular velocity of such neutron stars. In the Newtonian approach, this limit is obtained using

$$v_{\text{escape}} = \sqrt{\frac{2GM}{R}} \quad (48)$$

where G is the gravitational constant, M is the mass of the neutron star and R is the radius of the neutron star. Equation (48) gives

$$\Omega_{\text{Kepler}(N)} = 1.6\sqrt{\pi G \bar{\rho}} \quad (49)$$

while general relativistic corrections give

$$\Omega_{\text{Kepler}(GR)} = \frac{2}{3}\sqrt{\pi G \bar{\rho}} \quad (50)$$

Assuming a solid neutron star without differential rotation of uniform average density $\bar{\rho}_{ns} = 5.5 \times 10^{17} \text{ kg m}^{-3}$ we find that newborn neutron stars can reach angular velocities of $\Omega_{ns} = 7.2 \times 10^3 \text{ rad s}^{-1}$ without falling apart due to centrifugal forces.

In general relativistic models with differential rotation (Dimmelmeier et al. 2008) the iron cores of supernova progenitor stars may rotate at angular velocities in the range of $0.45 - 13 \text{ rad s}^{-1}$ ($\Omega_{\text{Kepler}(GR)} \simeq 6.7 \text{ rad s}^{-1}$ for an iron core with mass $M = 1.4$ solar masses and radius $R = 1.0 \times 10^3 \text{ km}$). Using conservation of angular momentum we get

$$\Omega_{ns} = \left(\frac{M_{ic}}{M_{ns}}\right) \left(\frac{R_{ic}}{R_{ns}}\right)^2 \Omega_{ic} \quad (51)$$

From (Dimmelmeier et al. 2008) we find that the iron cores of supernova progenitors have masses in the range of $1.2 - 1.8$ solar masses and radii from $1.0 \times 10^3 \text{ km}$ to $2.5 \times 10^3 \text{ km}$. Substituting, $\Omega_{ic} = 1.0 \text{ rad s}^{-1}$, $M_{ic} = M_{ns} = 1.4$ solar masses, $R_{ic} = 1.0 \times 10^3 \text{ km}$ and $R_{ns} = 12 \text{ km}$, we find that the angular velocity of a new-born neutron star is about $6.9 \times 10^3 \text{ rad s}^{-1}$. This is consistent with the $7.0 \times 10^3 \text{ rad s}^{-1}$ upper limit found by Hashimoto in 1994 (Hashimoto et al. 1994).

Simulating the angular momentum evolution of massive stars (8 – 25 solar masses) in their spherically symmetric models Heger et al. presented the first rotating presupernova stellar models that included a 1-dim prescription for angular momentum transport and centrifugal effects (Heger et al. 2000). These authors estimated the neutron star angular velocity by assuming that the total angular momentum contained in the pre-collapse iron core is conserved during collapse and supernova phases and is deposited completely in a rigidly rotating neutron star of radius equal to $\sim 12 \text{ km}$ and moment of inertia given by $0.35 M_{ns} R^2$ (Ott et al. 2006; Lattimer & Prakash 2001). In this way, they estimated an initial neutron star angular velocity of $6.3 \times 10^3 \text{ rad s}^{-1}$ for their fiducial 20 solar masses (zero age main sequence) stellar model.

8.2. Possible mechanisms responsible for the neutron star spin-down

According to the observational data, the angular velocities of neutron stars range between $\sim 1.0 \text{ rad s}^{-1}$ to $\sim 1.0 \times 10^4 \text{ rad s}^{-1}$. Typical (generic pulsar) neutron stars have angular velocities from $\sim 20 \text{ rad s}^{-1}$ to $\sim 3.0 \times 10^2 \text{ rad s}^{-1}$. The highest of these is up to a factor of 24 less than the theoretical upper bound of the initial angular velocity of the newborn neutron star. Several suggested processes that could lead to an early spin-down of a newborn (proto)neutron star include (Ott et al. 2006):

- (a) angular momentum redistribution by global hydrodynamic angular instabilities
- (b) r-modes and gravitational radiation back-reaction
- (c) rotation-powered explosions
- (d) viscous angular momentum transport due to convection
- (e) neutrino viscosity or dissipation of shear energy stored in differential rotation
- (f) magneto-centrifugal winds
- (g) early magnetic dipole radiation
- (h) late-time fall-back and

(i) anisotropic neutrino emission

It is also possible that slowly spinning cores are the natural end-product of stellar evolution. Angular momentum transport via magnetic processes yields angular velocities equal to $\sim 6.0 \times 10^{-2} \text{rads}^{-1}$ (Spruit & Phinney 1998) that is too low to explain the observational data. The authors had to rely on subsequent spin-up by off-center birth kicks to obtain angular velocities of $\sim 3.0 \text{rads}^{-1}$ to match the observations. Heger et al. followed a similar approach for magnetic angular momentum transport during stellar evolution to obtain neutron star angular velocities of $\sim 9.0 \times 10^2 \text{rads}^{-1}$ (Heger et al. 2003). Having in mind that stellar evolution theories with rotation are still improving and given the uncertainties in iron core angular velocities and angular momentum profiles we should be very careful in accepting any spin-down mechanism as the final theory.

In this paper we assumed that the neutron star is born with initial angular velocities of up to $\Omega_{n,s} \simeq 7.2 \times 10^3 \text{rads}^{-1}$ and the neutron star has a temperature range that allows the r-mode gravitational instability to survive. Since the rotational energy of the neutron star is the energy source of the r-mode oscillations, the emission of r-mode gravitational radiation is assumed to be responsible for the decreasing rotational energy of the neutron star.

9. WAVEFORM PARAMETERS: RANGE OF POSSIBLE VALUES OF α

In this section we determine (by doing a thorough examination of the literature review) the highest theoretically permitted value of α . The value of α has been the subject of many debates since the earliest work on r-mode gravitational waves. Here we present several contradictory results that were published during the last 15 years about the maximum possible value of α . The still ongoing debate on the subject made our choice of range of values of α a little tricky.

9.1. *Historic perspective of the r-mode saturation mechanism*

The hypothesis that newborn neutron stars may spin down due to r-mode gravitational radiation was based on three major discoveries:

- (a) The existence of a secular instability in rotating Jacobian ellipsoids describing an increase in the angular velocity due to gravitational radiation (Chandrasekhar 1970).
- (b) The proof that non-axisymmetric modes of the form $e^{im\phi}$ (ϕ being the azimuthal angle) for *all* rotating stars are driven towards instability by gravitational radiation reaction (Friedman & Schutz 1978a,b). This instability is known as the Chandrasekhar-Friedman-Schutz (CFS) instability.
- (c) The discovery of non-radial low frequency oscillation modes on white dwarfs similar to the Rossby waves (hence the name r-modes) in the Earth's oceans and

atmosphere (Papaloizou & Pringle 1978).

Though some work on r-mode oscillations on neutron stars was done during the 1980's (Saio 1982; Wagoner 1984) it wasn't until 1998 that it was demonstrated that neutron star r-mode oscillations satisfy the requirements for the CFS instability (Lindblom et al. 1998). Lindblom et al. showed that r-modes belong to the group of non-axisymmetric modes that can be driven unstable due to gravitational radiation. This theory predicted that (assuming the r-mode oscillation amplitude grows sufficiently large) r-mode gravitational radiation (primarily in the $m = 2$ harmonic) would carry away most of the angular momentum of a rapidly rotating newborn neutron star in the form of r-mode gravitational radiation.

In the early years after the discovery of the r-mode instability, initial scenarios assumed that the r-mode amplitude would grow to order unity (Lindblom et al. 2002) before some unknown process would saturate the mode (Porquet & Dubau 1999; Andersson & Kokkotas 2001). However, there were speculations that some non-linear hydrodynamics of the star might limit the growth of the r-mode to very small values. This could be the result of r-mode oscillations leaking energy (due to non-linear couplings) into other inertial modes faster than gravitational radiation reaction force could restore it. Since 1998 several studies on the saturation mechanism showed a variety of results.

Early work (Lindblom et al. 2000) showed that the hypothesis of r-mode gravitational radiation cannot be applied to cold ($T < 10^8 \text{°K}$) neutron stars whose crust is not in a fluid state. It was shown that in neutron stars colder than 10^8°K the crust might be perfectly solid and that would completely suppress the r-mode instability. However, the question about the r-mode amplitude growth and saturation on hot ($T > 10^8 \text{°K}$) neutron stars remained open.

In the absence of any saturation mechanism the r-mode amplitude would grow to values of order 1. This idea was supported by early relativistic simulations that showed that on a fixed neutron star geometry no r-mode amplitude saturation occurs even at large amplitudes (Stergioulas & Font 2001). These findings were further reinforced by the results of fully non-linear, 3-dim numerical simulations based on Newtonian hydrodynamics and gravitation. This study investigated the growth of the r-mode and found that the r-mode amplitude reached values of order 1 (Lindblom et al. 2001, 2002). However, both Newtonian and relativistic 3-dim hydrodynamical simulations were (and still are) severely limited by computational time and cannot probe the timescales on which r-modes may saturate. To bypass this limitation Lindblom et al. used artificially enhanced gravitational radiation force (increased by a factor of 4500) in order to evolve the r-mode amplitude and allow it to reach values of order 1.

Later on the problem was attacked analytically with the use of a weakly non-linear perturbation theory to study the non-linear interactions of the r-modes with

other inertial modes (Schenk et al. 2002; Arras et al. 2003; Brink et al. 2004). Calculations on a network of ~ 5000 modes with about 1.3 million couplings showed that the r-mode amplitude saturated at small values of order 10^{-4} . Furthermore, they showed that under some circumstances, it is possible to show that the r-mode amplitude evolution is dominated by just one three-mode coupling (r-mode plus 2 daughter modes).

The triplet of r-mode plus the 2 daughter modes, together with assumptions on the neutron star cooling mechanism and hyperon bulk viscosity, was used in further work on the r-mode instability: (a) describing the rotational frequency evolution of accreting neutron stars (Bondaescu et al. 2007) and (b) model the spin-down of a newborn neutron star by the emission of r-mode gravitational radiation (Bondaescu et al. 2009). The work on (a) showed that accreting neutron stars undergo a cyclic thermal runaway evolution during which the r-mode amplitudes remain saturated at values of order 10^{-5} while work on (b) showed that the r-mode amplitudes in newborn neutron stars saturate at values of order 10^{-4} to 10^{-2} .

Using a single triplet of modes, the lowest parametric instability threshold is very sensitive to the internal neutron star physics. The authors considered a model with a neutrino cooling mechanism, via a combination of fast and slow processes, viscous heating due to hyperon bulk viscosity and spin-down due to gravitational radiation and magnetic dipole radiation. Two necessary assumptions (that are also limitations) of this single-triplet model and were made so that r-mode amplitude saturation is achieved are: (a) high hyperon bulk viscosity and (b) fast neutrino cooling mechanism. The fast neutrino cooling assumes certain restrictions on the equation of state of the neutron star matter that may not be true for every neutron star. For example fast neutrino cooling by direct Urca-like processes requires exotic phases of matter in the core of neutron stars (Yakovlev & Pethick 2004; Yakovlev et al. 1999). Furthermore, if real neutron stars have low hyperon bulk viscosity the energy dissipated by the single triplet of modes used in (Bondaescu et al. 2007, 2009) may not be sufficient to stop the growth of the r-mode amplitude.

If the Bondaescu et al. assumptions for the neutron star model (based on the single triplet of modes) are not satisfied, several triplets of modes may be required to saturate the r-mode amplitude. In that case, several parametric instability thresholds would be passed before saturating the r-mode amplitude thus making it not clear at what order the latter would saturate. If the r-mode amplitude passes its first parametric instability threshold value, other near-resonant inertial modes are expected to be excited (via energy transfer from the r-mode) signaling the importance of non-linear effects (Bondaescu et al. 2009). This is a fundamental property of inertial modes which does not depend on the details of the equations of state or on a slow-rotation approximation. The r-mode frequencies reside inside an extended region where there is a sufficiently large number of inertial modes with similar frequencies, so it

is easy for resonance conditions to be satisfied.

Even if several multiple triplets of modes are included in simulating the non-linear effects, depending on how reliable the mode-coupling estimates of the r-mode saturation amplitude is, it may not be certain that the energy transfer to inertial modes will stop the instability at low r-mode amplitudes. If the mode-coupling mechanism does not saturate the growth of the r-mode early enough Bondaescu et al. pointed out that other mechanisms like suprathreshold bulk viscosity might then become relevant. The current scientific consensus is that the mode-couplings saturating the amplitude of the r-mode is a fundamental result and will remain valid even with an improved understanding. Nevertheless, it is thought very unlikely that the r-mode amplitude could grow larger than 10^{-1} .

In the absence of experimental evidence several authors still entertain the idea of r-modes saturating at amplitudes of order equal to or greater than 10^{-1} . It was shown that if the non-linear coupling mechanism does not come into play the r-mode amplitude would keep rising exponentially and eventually reach the suprathreshold regime (where the chemical equilibrium becomes greater than $K_B T$). In this high r-mode amplitude regime, the damping due to (suprathreshold) bulk viscosity increases dramatically (non-linearly) with increasing r-mode amplitude. This causes the viscous damping to overcome the gravitational instability and saturate the r-mode at amplitudes of order $10^{-1} - 1$ (Alford et al. 2012).

Considering the results found by the above studies it seems that the most likely values the r-mode amplitude may saturate at is anywhere between 10^{-4} to 10^{-1} . In our sensitivity study we considered r-mode waveforms of three saturation amplitudes 10^{-3} , 10^{-2} and 10^{-1} . Considering the worst case scenarios (that r-mode amplitudes saturate at values less than 10^{-2}) our best chances to settle this open question is to design a targeted search of r-mode gravitational waves from newborn neutron stars. This requires some waiting time and some preparation in order to be ready for the next local group supernova.

10. GRAVITATIONAL WAVE DETECTORS AND SIMULATED WAVEFORMS

In this section we discuss the sensitivity level of the aLIGO and ET detectors. We also present several plots of the frequency evolution dependence on f_o and α (according to the Owen et al. '98 model) and how these waveforms are used to construct the signals that were injected into the time-shifted data.

10.1. *Sensitivity of the gravitational-wave interferometers*

The past decade has seen the development of a worldwide network of gravitational-wave interferometers. The initial LIGO detectors achieved design strain sensitivity of $\sim 2 \times 10^{-23} \text{ Hz}^{-1/2}$ in the most sensitive frequency range of 100 – 130 Hz. The next generation of interferometers such as aLIGO and advanced Virgo (aVirgo) are expected to begin taking data starting in early Fall 2015.

The upgraded aLIGO/aVirgo experiments are expected to achieve a factor of ten higher strain sensitivity than initial LIGO/Virgo. In our simulation study below we show that aLIGO can probe r-mode gravitational-wave spin-down signals to newborn neutron stars within the Local Group of galaxies.

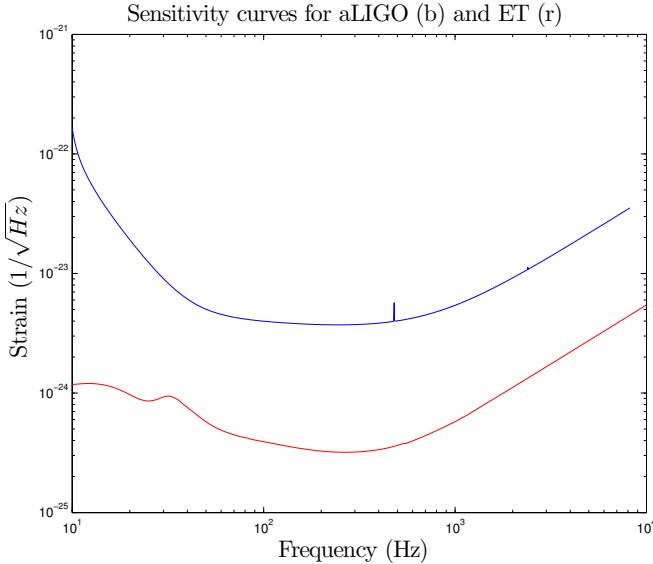


FIG. 6.— The sensitivity curves of aLIGO and ET: aLIGO simulated noise shows a maximum sensitivity of $\sim 5 \times 10^{-24} \text{ Hz}^{-1/2}$ at 110 – 130 Hz while ET simulated noise shows a maximum sensitivity of $\sim 2 \times 10^{-25} \text{ Hz}^{-1/2}$ at 110 – 130 Hz.

10.2. Choice of parameter values and waveform simulation

The Owen et al. '98 model was used to produce the waveforms injected in the MC and eLIGO noise colored with the aLIGO sensitivity curve and also the eLIGO noise colored with the ET sensitivity curve. In this model there are two parameters: the initial frequency f_o and the saturation amplitude α . We assume that the gravitational-wave frequency of the signal is between 600 – 1600 Hz (as shown in table 1). We also assume that the signal will be powerful enough for detection for at least 2500 s. This signal duration is enough for the power to drop to 17% of its initial value for waveforms with highest f_o and α values. However, the power drops only to 87% of the initial value for waveforms with the lowest f_o and α values. In the latter case, longer durations would be required to increase the SNR of the signal (when clustering pixels in the detection algorithms) and hence increase the detection distance. However, using 2500 s duration and 600 – 1600 Hz frequency span results in ft-maps of 2.5×10^6 pixels. To run the background and sensitivity study algorithms and to create ft-maps of this size requires memory that approaches the memory limitations of conventional CPUs.

We used three f_o values (700, 1100, 1500 Hz) and three α values (10^{-3} , 10^{-2} , 10^{-1}) resulting in nine waveforms. The dependence of the waveforms on f_o and α are shown in Fig.7 and Fig.8

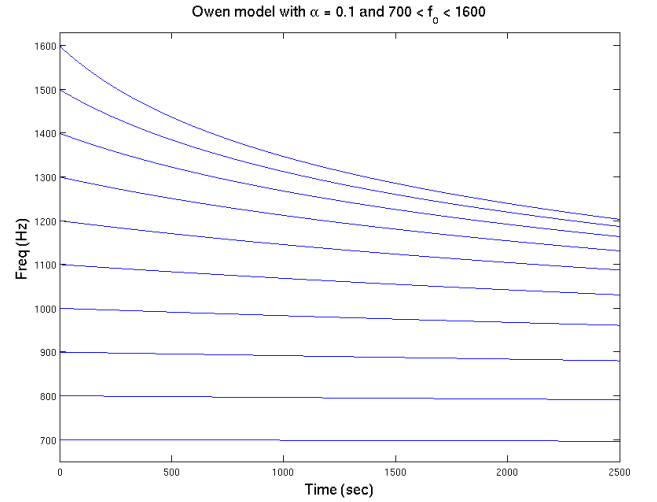


FIG. 7.— Frequency evolution dependence on the initial frequency f_o . The higher the f_o value the steeper the spin-down.

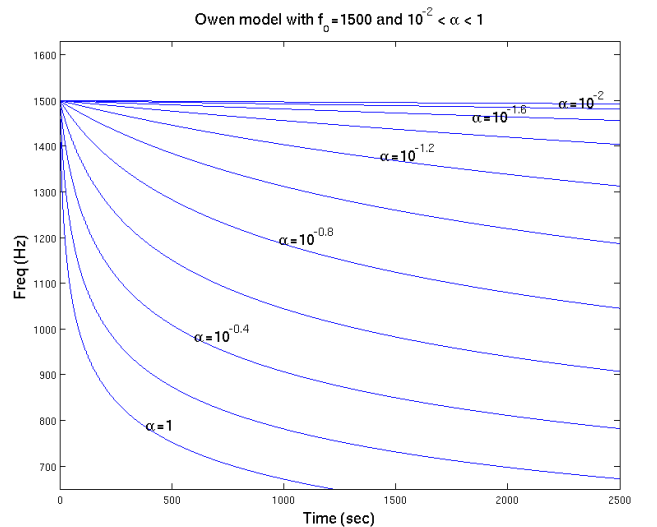


FIG. 8.— Frequency evolution dependence on the saturation amplitude α . The higher the α value the steeper the spin-down.

A gravitational wave emitted by a neutron star is a linear combination of the two polarizations, h_+ and h_\times and can be expanded in the detector's frame like (Owen 2010)

$$h(t) = F_+(t, \psi)h_+(t) + F_\times(t, \psi)h_\times(t) \quad (52)$$

where the coefficients $F_+(t, \psi)$ and $F_\times(t, \psi)$ are the detector antenna pattern functions for the two polarizations, t is the time in the detector frame and ψ is the polarization angle. The waveforms for the two polarizations are given by

$$h_+(t) = h_o \left(\frac{1 + \cos^2 \theta}{2} \right) \cos \Phi(t) \quad (53)$$

and

$$h_\times(t) = h_o \cos(\theta) \sin \Phi(t) \quad (54)$$

where h_o is the corresponding gravitational-wave strain

amplitude as measured on Earth, θ is the inclination angle and $\Phi(t)$ is the time dependent phase of the gravitational wave in the detector's frame and is given by

$$\Phi(t) = \Phi(t_0) + \Delta\Phi = \Phi(t_0) + \int_{t_0}^t 2\pi f_{gw}(t') dt' \quad (55)$$

where t_0 is the fiducial start time of the observation and f_{gw} is the gravitational wave frequency in the detector's frame. The angle θ can be set equal to zero by assuming that the direction of propagation of the gravitational wave is perpendicular to the plane of the interferometer.

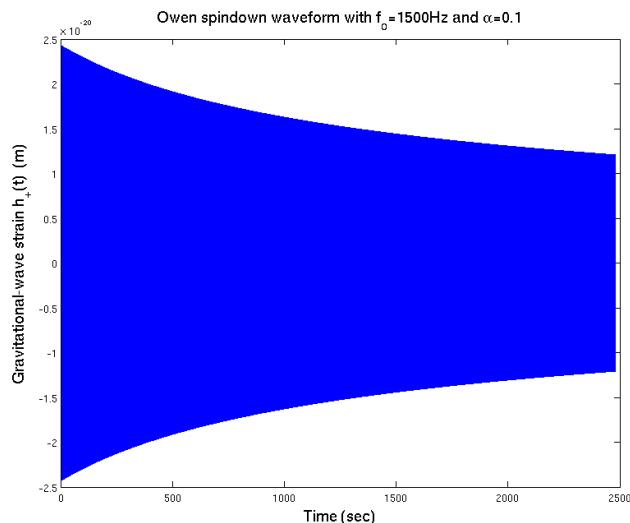


FIG. 9.— This is an example of a $h_+(t)$ gravitational-wave strain that was injected in simulated aLIGO and ET noise.

11. INJECTION RECOVERY AND DETECTABILITY

This section starts with a discussion on matched filtering, the optimal detection algorithm. This algorithm requires accurate knowledge of the signal we are searching for. Though this is not the case for the r-modes (due to the wide range of possibilities for the parameter values) matched filtering gives theoretical upper bounds and a measure of evaluating the efficiency of the clustering algorithm used in our present sensitivity study. Our study is designed to assess the detectability of r-mode gravitational wave signals injected on (time-shifted) data colored with the sensitivity curves of aLIGO and ET gravitational wave detectors. Focusing on realistic excess cross-power searches, we show that second-generation detectors such as advanced LIGO (aLIGO) may be able to probe neutron star spin-down models out to astrophysically interesting distances of ~ 1 Mpc. Third generation detectors such as Einstein Telescope (ET) may be able to probe such signals out to distances of ~ 10 Mpc.

11.1. Matched filtering estimates

For gravitational-wave signals of a known form, the theoretically optimal search strategy is matched filtering

(Owen & Sathyaprakash 1999). However, the r-mode signals we consider here are not suitable for a search with a matched filtering detection algorithm due to the lack of accurate models that are available to generate r-mode waveforms. A search with matched filtering must include a template bank that spans the space of all possible signals and unknown parameter values. An incomplete template bank can result in faulty upper limits if the true signal falls outside the template space. In order to generate a complete template bank, we require firm knowledge of the details of the waveform's phase evolution. In presenting the above model, we have not aspired to this degree of accuracy. Moreover, even if a complete and accurate model could be written down, there may be computational challenges associated with performing the search, especially for long signals with many parameters.

Nonetheless, it is useful to compare the detection distances calculated using the excess-power technique to estimates for what can be achieved with matched filtering as this places an upper limit on the detection distance that can be achieved through improvements to the data-analysis scheme. As before, we assume optimal orientation of the source, optimal orientation of the detector network, a false-alarm probability $\leq 0.1\%$ and a false dismissal probability $\leq 50\%$. We find that highly idealized matched filtering allows us to extend the detection distance up to factors of 10 - 20 as shown in table 1. This factor varies depending in part on the efficiency of the pattern recognition algorithm for different signal types.

11.2. Spectrograms and the seedless clustering detection algorithm

To estimate the distances at which we can see the signals predicted by the Owen et al. '98 model using various combinations of the model parameters (f_0, α), we simulate an excess cross-power search for long-lived gravitational waves associated with a well-localized electromagnetic counterpart, in the r-mode case this would be a supernova explosion. This simplifies the search to a single direction, although these techniques may be extended to all-sky searches in the future.

Within this $2500 \text{ s} \times 1000 \text{ Hz}$ on-source region, and following (Thrane et al. 2011), we create a spectrogram of signal-to-noise ratio $\text{SNR}(t; f)$, which is proportional to the cross-correlation of the H1 and L1 strain data. Here f refers to the frequency bin in a discrete Fourier transform centered on time t . We use 1s-long, 50%-overlapping, Hann-windowed data segments, which yield spectrograms with a resolution of $0.5 \text{ s} \times 1 \text{ Hz}$. The signal to noise ratio is given by

$$\langle \text{SNR}(t; f) \rangle = h_0^2 (1 - \cos^2 \iota), \quad (56)$$

where ι is the angle between the direction of propagation of the gravitational wave and the plane of the interferometer (the noise fluctuations can be both positive and negative). A formal derivation of $\text{SNR}(t; f)$ can be found in (Thrane et al. 2011). An example of a $\text{SNR}(t; f)$ spectrogram with a r-mode injection added to simulated

detector noise can be seen in Fig.10. The problem of detection is to identify a track of positive-valued pixels in the presence of noise.

In our simulation, we use a network consisting of two 4km LIGO observatories assumed to be operating at aLIGO design sensitivity; one in Hanford (H1) and one in Livingston (L1). We create a spectrogram of signal-to-noise ratio $\text{SNR}(t;f)$ in our $2500\text{s} \times 1000\text{Hz}$ on-source region, which is proportional to the cross-correlation of the H1 and L1 strain data.

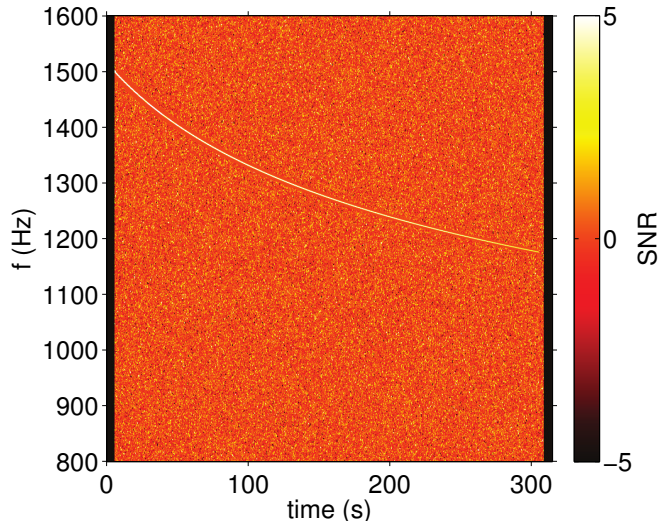


FIG. 10.— Injection of a r-mode signal using a waveform of $f_o = 1500\text{Hz}$ and $\alpha = 0.1$ at a distance of 1Kpc. The background was simulated using MC data colored with the aLIGO sensitivity curve.

To recover the injected signals, we apply a seedless clustering algorithm (Thrane & Coughlin 2013) that looks for clusters of positive pixels. The pixels are combined to determine the SNR for the entire cluster denoted by $\text{SNR}(c)$ which is distinct from $\text{SNR}(t;f)$ associated with individual pixels in a spectrogram. To form the SNR for the cluster the pixels are summed using their individual sigmas as weights.

The algorithm was applied to Monte Carlo Gaussian noise colored with the aLIGO sensitivity curve, eLIGO S5 data (noise) recolored with the aLIGO sensitivity curve and Monte Carlo Gaussian noise colored with the ET sensitivity curve (Fig.6). The algorithm was used in order to determine the threshold for an event with false alarm probability $\leq 0.1\%$. For the MC data colored with the aLIGO sensitivity curve we found the cluster SNR threshold to be 7.2 while using the ET sensitivity curve we found the cluster SNR threshold to be 8.1.

We then injected simulated signals into the Monte Carlo noise at varying distances. We determined the distance above which 50% of the signals are recovered, which corresponds to the distance at which we can observe a signal with false alarm probability $\leq 0.1\%$ and false dismissal probability $\leq 50\%$. These detection distances are shown in table 1 for all 9 different combinations of parameters.

When testing the sensitivity of a given detection algorithm, we run the algorithm on 10^3 noise maps and out of those we set the highest (cluster) SNR as the SNR threshold. This threshold corresponds to a fixed gravitational-wave strain, $h_o = h_{th}$. Using (14) and this threshold h_{th} , we can test what combination of parameters α and f_o and at what distance d the corresponding waveform can be detected. Substituting h_o with h_{th} and solving (14) for d we get the distance expression in units of Mpc

$$d \approx 1.5 \times 10^{-23} \left(\frac{f}{1\text{kHz}} \right)^3 \frac{|\alpha|}{h_{th}} \quad (57)$$

where

$$f^3 \sim (1 + 10^{-20} |\alpha|^2 f_o^6 t)^{-\frac{1}{2}} \quad (58)$$

Equations (57) and (58) suggest that (for a given value of h_{th}) knowing the detection distance d_1 for one waveform of parameters (α_1, f_{o1}) we can estimate the expected distance for another waveform of parameters (α_2, f_{o2}) using

$$d_2 \sim \frac{|\alpha_2|}{|\alpha_1|} \left(\frac{1 + \lambda |\alpha_1|^2 f_{o1}^6}{1 + \lambda |\alpha_2|^2 f_{o2}^6} \right)^{\frac{1}{2}} d_1 \quad (59)$$

where $\lambda \approx 10^{-20}t$. This suggests that when the parameters (α, f_o) are such that $\lambda |\alpha|^2 f_o^6 \ll 1$ then

$$d_2 \sim \frac{|\alpha_2|}{|\alpha_1|} d_1 \quad (60)$$

This is the case for $f_{o1} = 7 \times 10^2$, $\alpha_1 = 10^{-3}$ and $t = 2.5 \times 10^3$ giving $\lambda |\alpha_1|^2 f_{o1}^6 \approx 2.9 \times 10^{-6}$ and $f_{o2} = 7 \times 10^2$, $\alpha_2 = 10^{-2}$ and $t = 2.5 \times 10^3$ giving $\lambda |\alpha_1|^2 f_{o1}^6 \approx 2.9 \times 10^{-4}$. The seedless based algorithm gives for the first case a detection distance of 40 Kpc while for the second case it gives 4 Kpc according to (60).

For $\lambda |\alpha|^2 f_o^6 \simeq 1$ or $\lambda |\alpha|^2 f_o^6 \geq 1$ the detection distances our algorithm gives follow equation (59). For example for $f_{o1} = 1.5 \times 10^3$, $\alpha_1 = 10^{-1}$ and $t = 2.5 \times 10^3$ giving $\lambda |\alpha_1|^2 f_{o1}^6 \approx 2.9$ and $f_{o2} = 1.5 \times 10^3$, $\alpha_2 = 10^{-2}$ and $t = 2.5 \times 10^3$ giving $\lambda |\alpha_1|^2 f_{o1}^6 \approx 3 \times 10^{-2}$ we get the relation $d_2^{est} \approx 0.19d_1$. The detection distances d_1 and d_2 are related by $d_2 \approx 0.17d_1$ (column 2), $d_2 \approx 0.19d_1$ (column 3) and $d_2 \approx 0.18d_1$ (column 4) of table 1. Thus we conclude that the detection algorithm behaves in a way consistent with the theoretical predictions.

12. DISCUSSION

The most optimistic scenarios in the Bondarescu et al. numerical simulations show that r-mode gravitational-wave strains take values of $5 \times 10^{-25} \text{Hz}^{-1/2}$ at $f = 400\text{Hz}$ and $6 \times 10^{-24} \text{Hz}^{-1/2}$ at $f = 600\text{Hz}$ from sources that are 100 Kpc away from the detectors. Using (14) we can show that these strain amplitudes correspond to r-mode saturation amplitudes that range from $\alpha = 5.2 \times 10^{-2}$ to $\alpha = 1.9 \times 10^{-1}$. In the worst case scenarios their work shows that r-mode gravitational wave strains take values of $5 \times 10^{-26} \text{Hz}^{-1/2}$ at $f = 600\text{Hz}$ ($\alpha = 1.5 \times 10^{-3}$)

TABLE 1
SENSITIVITY STUDY USING A SEEDLESS CLUSTERING (SC) ALGORITHM AND MATCHED FILTERING (MF)

r-modes waveform (f_o, α) (Hz, unitless)	MC data aLIGO s.c./SC (Mpc)	eLIGO data aLIGO s.c./SC (Mpc)	MC data ET s.c./SC (Mpc)	MC data aLIGO s.c./MF (Mpc)
(1500, 0.1)	1.2	1.1	9.7	22
(1100, 0.1)	0.97	1.1	8.1	13
(700, 0.1)	0.44	0.42	4.3	4.8
(1500, 0.01)	0.19	0.21	1.8	2.9
(1100, 0.01)	0.13	0.12	1.1	1.3
(700, 0.01)	0.040	0.043	0.39	0.54
(1500, 0.001)	0.016	0.021	0.16	0.35
(1100, 0.001)	0.014	0.012	0.11	0.19
(700, 0.001)	0.0040	0.0044	0.039	0.048

^a Distances are calculated for a false alarm probability $\leq 0.1\%$ and a false dismissal probability $\leq 50\%$ using Monte Carlo (MC) aLIGO noise and MC ET noise.

^b Doing a background study on 1000 maps the cluster SNR threshold was estimated to be $SNR_{th} = 7.2$ with the aLIGO sensitivity curve (s.c.) and $SNR_{th} = 8.1$ with the ET s.c. Sources are assumed to be optimally oriented.

^c Columns 2, 3 and 4 are the distances at which 50 out of 100 injections were recovered using the SC algorithm and column 5 shows the corresponding distances using a highly idealized MF.

to $2 \times 10^{-27} \text{ Hz}^{-1/2}$ at $f = 350 \text{ Hz}$ ($\alpha = 3.1 \times 10^{-4}$). Clearly, our results show that we can only be hopeful for a large α r-mode gravitational wave detection.

In the non-linear bulk viscosity mechanism of Mark Alford et al. the r-mode amplitudes grow up to values of orders $10^{-1} - 1$. A 1 KHz gravitational-wave signal generated by r-mode oscillations saturated at these amplitudes will create gravitational-wave strain values from 10^{-24} to 10^{-23} respectively at distances of 1 Mpc where the supernova rate is about 3-4 per century. The same wave at a distance of 10 Mpc where the supernova rate is at about 1-2 per year (Mannucci et al. 2008) will have a strain value of order 10^{-25} to 10^{-24} . Our sensitivity results show that we can exclude the O(1) r-mode oscillations by the absence of any r-mode detections at those distances.

Our results show that for a 1 KHz gravitational wave generated by a r-mode oscillation saturated at an amplitude of order 10^{-2} the maximum detection distance is 0.1 Mpc. The result for a gravitational wave of the same frequency but generated by a r-mode oscillation saturated at an amplitude of order 10^{-1} is a maximum detection distance of 1 Mpc. These results show that our search method can detect gravitational-wave strains of order down to 10^{-24} . The sensitivity curve of aLIGO at 1 KHz is about $5 \times 10^{-24} \text{ Hz}^{-1/2}$ showing that with our current algorithms we can detect signals that are 5 times weaker than the noise.

Detecting a gravitational-wave strain of order 10^{-24} gives information about the ratio α/d and does not specify the value of α . Therefore, to determine the value of α we need an electromagnetic trigger to provide the distance for us. Given the distance we can then calculate the value of the saturation parameter, α . A detection of r-mode gravitational radiation coming from a supernova is the best possible outcome of our efforts in this search. However, a non-detection can also be useful in determining an upper limit on the r-mode saturation amplitude and disprove the theories that suggest scenarios of r-mode saturation amplitudes

higher than that.

Initially, this project started with the target to design a search that would set an upper bound on the saturation amplitude of the r-mode mass current oscillations on neutron stars. For this work we used the Owen et al. '98 model that assumes a polytropic equation of state (EOS). Therefore, our work was initially based on a specific EOS, using specific values for \tilde{J}_2 and \tilde{I} giving $Q \sim 0.094$. However, we may use different EOS and using the integrals for \tilde{J}_2 and \tilde{I} we can calculate their corresponding Q value and therefore, the corresponding waveforms. Therefore, a hypothetical r-mode gravitational wave detection can not only settle the debate on the r-mode oscillations saturation amplitude but also impose severe constraints on the EOS of the matter in the core of a neutron star.

In the Owen et al. '98 model, non-linear couplings between the r-mode and other inertial modes as well as strong magnetic fields (crucial in the evolution/saturation of the r-mode amplitude) were not explicitly modeled. However, when compared to the complicated numerical simulations in Bondarescu et al. we got a significant overlap for the r-mode gravitational wave frequency evolution during the first two weeks after the neutron star is born. This is the era of a neutron star's life we are interested in.

An improved model that includes magnetic fields effects can be found in (Staff et al. 2012). This work considers the same Owen et al. '98 model but with an additional frequency damping term due to magnetic braking. The restrictions their findings imply are that the r-modes may be dominant only for B-fields of magnitude below 10^{13} G . This result does not impose any changes on the r-mode gravitational waveforms. It merely says that we shouldn't be hopeful to observe r-mode gravitational radiation in neutron stars with very strong magnetic fields. On the other hand, this magnetic braking restriction is dependent on the equation of state, hence not very decisive on the magnitude of the magnetic fields for which we should not hope to

detect r-mode gravitational waves.

The accuracy of the waveforms determines the type of decision making algorithm we should be using when searching for a signal. Lack of reliable models of the physical system implies production of unreliable waveforms. This is the reason we did not search for the r-mode signal using matched filtering. The algorithms we used in this study are based on the statistical significance of signal to noise ratios of clusters made of pixels above a certain snr threshold. This method did not use any knowledge of the signal. Knowledge of the r-mode signal can be used and make minor modifications in our existing algorithms, however, there was not much hope for a dramatic improvement in sensitivity. We were still able to recover signals of one order of magnitude weaker than the noise. We are currently considering algorithms designed to search for specific signals, in our case the r-mode. We hope that customizing the search algorithm for a specific signal can significantly increase the sensitivity in decision making.

An ideal class of decision making algorithms, which are suitable specifically for cases when the signal is not precisely (but only crudely) known, is provided by machine learning algorithms (MLAs). Three classes of MLAs we are currently exploring are artificial neural networks (ANN), support vector machines (SVM) and local space classifiers (LSC). MLAs are considered novel methods of signal recognition in the area of gravitational-wave searches. We are now working on developing r-mode search algorithms using the above three techniques. Currently, we are producing data in the parameter space of interest. The plan is to repeat the same sensitivity study we presented in this paper using MLAs for decision making/recognition of the desired signals. The results will be compared to our present results and published in a future paper.

13. CONCLUSIONS

(a) In the worst case scenario of Bondarescu et al. , $\alpha = 10^{-4} - 10^{-3}$. If this is correct the results from our sensitivity study show that we can only be hopeful (with this search method) to detect r-mode gravitational radiation from sources that are up to 21 Kpc away.

(b) If the best case scenario of Bondarescu et al. (with $\alpha = 10^{-1}$) prevails then we can be hopeful to detect r-mode gravitational radiation from sources that are up to 1100 Kpc away. In this case it may not be possible to distinguish whether it is Bondarescu et al. or Alford et al. mechanism that comes into play.

(c) To exclude the validity of Bondarescu et al. results a r-mode gravitational wave detection yielding a value of $\alpha \geq 0.2$ is needed. In that case we will have strong indications that Alford et al. mechanism is the correct r-mode oscillation amplitude saturation mechanism.

(d) If the best case scenario (of high r-mode saturation amplitudes) is correct we may be able to detect r-mode gravitational radiation from a supernova event within our local group (~ 1 Mpc). Considering the low rate of the local group supernovae (3-4 per century) and that the latest supernova in the local group occurred in January 2014, we may have to wait another 25-30 years until the next one.

(e) The aLIGO and ET sensitivity results show that for large amplitudes of α , the detection distances are up to 1.1 Mpc (2-3 events per century) and 10 Mpc (1-2 events per year) respectively. Using aLIGO, to exclude saturation amplitudes of order 10^{-1} , a null result at a distance of ≤ 0.42 Mpc is required. Using ET, to exclude the same saturation amplitudes a null result at a distance of ≤ 4.3 Mpc is required. Considering the event rates at those distances we can only hope for such results only after several years of ET operation.

(f) We do not need all the complicated physics of the neutron star to approximate the r-mode waveforms during the first 2 weeks after the onset of the r-mode gravitational radiation. A model where high magnetic fields are excluded and details of the r-mode saturation mechanism are unknown can still give a good approximation of the r-mode waveforms during the early stages of gravitational radiation.

(g) When the model waveform parameters take values over large ranges, choosing a decision making algorithm may not be a simple task. Clustering algorithms may yield satisfactory results but that is not necessarily the best option we can have. Other techniques (for example MLAs) that do not require accurate knowledge of the waveform parameter values may result in longer detection distances. Increasing the detection distance by a factor of 2 or 3 can make the difference.

For lengthy discussions we thank: the Stochastic Transient Analysis Multi-detector Pipeline (STAMP) group that also developed the code we used, Ruxandra Bondarescu, Ira Wasserman, Mark Alford, Lee Lindblom, Kostas Kokkotas and Nick Stergioulas.

REFERENCES

- Alford, M. G., Mahmoodifar, S., & Schwenzer, K. 2012, Phys.Rev., D85, 044051
 Alford, M. G., & Schwenzer, K. 2012, PoS, ConfinementX, 258
 Andersson, N. 1998, Astrophys.J., 502, 708
 Andersson, N., & Kokkotas, K. D. 2001, International Journal of Modern Physics D, 10, 381
 Ando, S., Beacom, J. F., & Yuksel, H. 2005, Phys.Rev.Lett., 95, 171101
 Arras, P., Flanagan, E. E., Morsink, S. M., et al. 2003, Astrophys.J., 591, 1129
 Baumgarte, T., Teukolsky, S., Shapiro, S., Janka, H., & Keil, W. 1996, Astrophys.J., 468, 823
 Bondarescu, R., Teukolsky, S. A., & Wasserman, I. 2007, Phys.Rev., D76, 064019
 —. 2009, Phys.Rev., D79, 104003
 Branch, D., & Tammann, G. A. 1992, Annual Review of Astronomy and Astrophysics, 30, 359

- Brink, J., Teukolsky, S. A., & Wasserman, I. 2004, *Phys.Rev.*, D70, 121501
- Chandrasekhar, S. 1970, *Phys. Rev. Lett.*, 24, 611
- Clemens, J. C., & Rosen, R. 2004, *Astrophys.J.*, 609, 340
- de Araujo, J. C. N., Miranda, O. D., & Aguiar, O. D. 2005, *Class.Quant.Grav.*, 22, S471
- Dimmelmeier, H., Ott, C. D., Marek, A., & Janka, H.-T. 2008, *Phys.Rev.*, D78, 064056
- Dragicevich, P. M., Blair, D. G., & Burman, R. R. 1999, *Mon. Not. Roy. Astron. Soc.*, 302, 693
- Duncan, R. C. 1998, arXiv:astro-ph/9803060
- Ferrari, V., Miniutti, G., & Pons, J. A. 2003, *Mon.Not.Roy.Astron.Soc.*, 342, 629
- Friedman, J. L., & Morsink, S. M. 1998, *Astrophys.J.*, 502, 714
- Friedman, J. L., & Schutz, B. F. 1978a, *ApJ*, 221, L99
- . 1978b, *ApJ*, 222, 281
- Hashimoto, M.-A., Oyamatsu, K., & Eriguchi, Y. 1994, *ApJ*, 436, 257
- Heger, A., Langer, N., & Woosley, S. 2000, *Astrophys.J.*, 528, 368
- Heger, A., Woosley, S., Langer, N., & Spruit, H. 2003, arXiv:astro-ph/0301374
- Ho, W. C., & Lai, D. 2000, *The Astrophysical Journal*, 543, 386
- Kirshner, R. P., & Kwan, J. 1974, *ApJ*, 193, 27
- Kokkotas, K. D., & Andersson, N. 2001, arXiv:gr-qc/0109054
- Lattimer, J., & Prakash, M. 2001, *Astrophys.J.*, 550, 426
- Lattimer, J. M., & Prakash, M. 2007, *Phys.Rept.*, 442, 109
- Levin, Y. 1999, *The Astrophysical Journal*, 517, 328
- Li, Y.-S., & White, S. D. 2008, *Mon.Not.Roy.Astron.Soc.*, 384, 1459
- Lindblom, L., Owen, B. J., & Morsink, S. M. 1998, *Phys. Rev. Lett.*, 80, 4843
- Lindblom, L., Owen, B. J., & Ushomirsky, G. 2000, *Phys.Rev.*, D62, 084030
- Lindblom, L., Tohline, J. E., & Vallisneri, M. 2001, *Phys.Rev.Lett.*, 86, 1152
- . 2002, *Phys.Rev.*, D65, 084039
- Mannucci, F., Maoz, D., Sharon, K., et al. 2008, *Mon.Not.Roy.Astron.Soc.*, 383, 1121
- Ott, C. D., Burrows, A., Thompson, T. A., Livne, E., & Walder, R. 2006, *Astrophys.J.Suppl.*, 164, 130
- Owen, B. J. 2010, *Phys.Rev.*, D82, 104002
- Owen, B. J., Lindblom, L., Cutler, C., et al. 1998, *Phys.Rev.*, D58, 084020
- Owen, B. J., & Sathyaprakash, B. 1999, *Phys.Rev.*, D60, 022002
- Papaloizou, J., & Pringle, J. 1978, *Mon.Not.Roy.Astron.Soc.*, 182, 423
- Porquet, D., & Dubau, J. 1999, arXiv:astro-ph/9912065
- Rezania, V., & Jahan-Miri, M. 2000, *Mon.Not.Roy.Astron.Soc.*, 315, 263
- Saio, H. 1982, *ApJ*, 256, 717
- Schenk, A. K., Arras, P., Flanagan, E. E., Teukolsky, S. A., & Wasserman, I. 2002, *Phys.Rev.*, D65, 024001
- Schmidt, B. P., Kirshner, R. P., Eastman, R. G., et al. 1994, *ApJ*, 432, 42
- Shibata, M., & Uryu, K. 2000, *Phys.Rev.*, D61, 064001
- Spruit, H., & Phinney, E. 1998, *Nature*, 393, 139
- Staff, J. E., Jaikumar, P., Chan, V., & Ouyed, R. 2012, *The Astrophysical Journal*, 751, 24
- Stergioulas, N., & Font, J. A. 2001, *Phys.Rev.Lett.*, 86, 1148
- Thrane, E., & Coughlin, M. 2013, arXiv:1308.5292
- Thrane, E., Kandhasamy, S., Ott, C. D., et al. 2011, *Phys.Rev.*, D83, 083004
- Wagoner, R. V. 1984, *ApJ*, 278, 345
- Yakovlev, D., Levenfish, K., & Shibano, Y. 1999, *Phys.Usp.*, 42, 737
- Yakovlev, D. G., & Pethick, C. 2004, *Ann.Rev.Astron.Astrophys.*, 42, 169